



DIFFERENTIAL ANALYSIS OF HUMAN KIDNEY STONE SAMPLES USING SEGMENTATION

V.ELUMALAI,MR.SVIJAYARAGHAVAN.

Ecturer in electronics and communication engg.

Sri chandrasekharendra saraswathi viswa mahavidyalaya,enethur,kanchipuram ,

Email :elumalai.be08@yahoo.com , professorvijay@gmail.com

ABSTRACT

To establish a sensitive method based on widely used electro spray ionization mass spectrometry (ESI-MS) for diagnosis of melamine-induced kidney stones and to probe the differential formation of melamine-induced kidney stones at molecular levels. Human kidney stones were collected in hospital from 6 groups of patients at different ages. ESI-MS was employed as the main technique with the principal component analysis for data processing. Using principal component analysis (PCA) of the ESI-MS fingerprints, a set of 21 melamine-induced kidney stone samples and 21 uric acid derived kidney stone samples were successfully differentiated from the other groups, rendering ESI-MS method a potential platform for differential analysis of the human kidney stones of various causes at molecular levels. The experimental results also indicate that in addition to the melamine, the chemical compounds enwrapped in the melamine-induced kidney stone samples are different from other kidney stone samples. These findings suggest that ESI-MS is a useful tool for diagnosis of melamine-induced kidney stone samples and the melamine-induced kidney stone could be formed by different mechanisms.

1. INTRODUCTION

Kidney stones, one of the most painful urologic disorders, have beset humans for centuries. It is estimated that about three percent of the world's population will suffer from kidney stones in their lifetime (Preminger GM (2010) [1]). Annually, about 3 million people need medical care due to kidney stone problems (Herring LC (1962) [2])). Kidney stones in human are normally caused by many factors, such as the diet and genetics (Citron JT(1996),Hiatt RA[3])). For example, it is known that the ingestion of melamine illicitly used in food may cause the formation of kidney stones in both humans (HuB,Peng XJ[4]) and animals (Jackson JE (1980) [5]). Although, the

formation mechanism for the melamine-induced kidney stones remains unclear, unambiguous chemical profiling of the melamine-induced human kidney stones is urgently required for better medical care performance. Chinese government covers all the medical expenditures for the melamine-induced kidney stone diseases after the melamine event, while patients suffering from uric acid-induced kidney stones are not included (Jia LQ, Shen Y, [6], MalekRS(1979)[7]). Thus, accurate detection of melamine-induced human kidney stones and the study of the formation mechanism as well are of great significance to both clinics diagnosis and economic interests.

Patientnumber	Age	Sex	Quantityand period	Stonelocation	Imagingstudies
Sample1	26 month	Male	30-50 g/day,2years	Leftureter	Nonopaquestone
Sample2	36 month	Female	30-50 g/day,1.5years	Leftkidneypelvis	Nonopaquestone
Sample3	7years	Male	30-50 g/day,2.5years	Leftkidneypelvis	Radiopaque
Sample4	17 month	Male	30-50 g/day,1.5year	Leftkidneypelvis	Radiopaque
Sample5	48years	Female	Nodrinking	Rightureter	Radiopaque
Sample6	44years	Male	Nodrinking	Leftkidneypelvis	Radiopaque

2. RELATED WORK

Evan AP, Coe FL, Liegeman JE, Worcester E et al, have proposed Persistent HBV replication in HBeAg-negative chronic hepatitis B may trigger strong immune responses against the virus and result in liver necroinflammation. Previous reports have indicated a close association of HBV replication after HBeAg seroconversion with the appearance of procore and basal core-promoter mutations as well as the severity of liver disease. In this study, there was no different prevalence of procore stop codon mutation between the different clinical stages of HBeAg-negative chronic HBV infection. Therefore, the appearance of procore stop codon mutation alone may play a minimal pathogenic role in chronic HBV infection. In contrast, the frequency as well as likelihood of basal core-promoter mutant increased with the progression of liver disease, implicating this mutant may play a major role in the pathogenesis of HBeAg-negative chronic hepatitis B. By using the logistic regression analysis, those patients with advanced age and with basal core-promoter mutant infection were at increased risk for the development of liver cirrhosis and HCC are showed. In addition, the prevalence of basal core-promoter mutant was significantly higher in younger patients with liver cirrhosis and HCC compared with age-matched inactive carriers is found. Therefore, the possibility of cohort effect of basal core-promoter mutant was not likely. These data regarding an association of basal core-promoter mutant with progression of chronic hepatitis and malignant transformation of liver cell may be reasoned by the alternation of amino acid sequences of the X protein that contributes to hepatocarcinogenesis. However, the major limitation of study was the cross-sectional design with all biological factors and disease status determined at the same time.

Moe OW et al, have proposed The formation of stones in the urinary tract stems from a wide range of underlying disorders. That clinician's look for the underlying causes for nephrolithiasis is imperative to direct management. There are many advances in genetics, path physiology, diagnostic imaging, medical treatment, medical prevention, and surgical intervention of nephrolithiasis. Here, a brief general background and focus mainly on path physiology and medical treatment of kidney stones provided. Although important advances have been made in understanding nephrolithiasis from single gene defects, the understanding of polygenetic causes of kidney stones is still largely elusive. A substantial proportion of data that resulted in new methods of treatment and prevention, which can be empirical or definitive, has focused on urinary luminal chemical composition of the precipitating solutes. Manipulation of inhibitors and epithelial factors is important and needs further investigation. Advances in

the management of nephrolithiasis depend on combined efforts of clinicians and scientists to understand the path physiology.

Otnes B et al, have proposed To evaluate the spectrum of urinary tract stone compositions in patients managed at one center. Methods: A total of 710 urinary calculi, passed spontaneously or after extracorporeal shock-wave lithotripsy as well as collected by endoscopic or open surgical procedures were analyzed by applying chemical and physicochemical methods primarily used for detecting minerals in our laboratory. Results: The distribution of stone compositions were noted as 454 (64.9%) calcium oxalate; 104 (14.6%) calcium phosphate; 99 (13.9%) struvite; 24 (3.3%) uric acid; 21 (2.9%) mixed; 5 (0.7%) cystine; and 3 (0.4%) xantine stones. Conclusion: Calcium stones, calcium oxalate in particular predominate among other types of urinary calculi in our center. Infection stones still have a considerable incidence that stays near to calcium phosphate calculi.

Sodhi RNS, Chen HW et al, have proposed Hepatitis (plural hepatitises) is a medical condition defined by the inflammation of the liver and characterized by the presence of inflammatory cells in the tissue of the organ. The name is from the Greek *hepar*, the root being *he pat*, meaning *liver*, and suffix *-itis*, meaning "inflammation. The condition can be self-limiting (healing on its own) or can progress to fibrosis.

Bankman I.N. et al, have proposed The result of this assessment demonstrated that "adding dynamic color to the facial expression synthesis is an effective way to express emotions in virtual facial images". On the other hand, all the previous research outcomes are similar in that they extracted the 2D facial features' expressions. Researchers have tried to improve the performance of the emotion recognition system. They suggested using the 3D geometric information for feature extraction and this approach has positively affected the performance. One of most effective approaches based on 3D geometric information has been applied.

Warfield, S.K., Zou, K.H., Wells, W.M et al, Accurate segmentation of different brain tissues is of much importance in magnetic resonance imaging. This paper presents a comparison of the existing segmentation algorithms that are deployed in the neuro imaging community as part of two widely used software packages. The results obtained in this comparison can be used to select the appropriate segmentation algorithm for the neuro imaging application of interest. In addition to the entire brain area, a comparison is carried out for the sub cortical region of the brain in terms of its gray matter composition. In applications where functional localization is of importance, knowing the precise location of a particular brain structure is a prerequisite to successful treatment. For instance, analysis prior to brain

surgery is done by experts who examine images of the brain and perform a manual segmentation of the structure of interest. However, there exists some disagreement and variability between different independent experts who perform manual segmentation on such images, indicating that there is still room for improvement in the segmentation process.

Comanicu and P. Meer et al, Segmentation of pathological space is a nontrivial problem. To improve the reliability of segmentation, 3D image denoising is often a necessary preprocessing step. So a novel 3D image denoising procedure based on local approximation of the edge surfaces using a set of surface templates is proposed. Followed by presented a new fully automated approach for segmentation of lungs with such high-density pathologies. Our method consists of two main processing steps. First, a novel robust active shape model (RASM) matching method is utilized to roughly segment the outline of the lungs. The initial position of the RASM is found by means of a rib cage detection method. Second, an optimal surface finding approach is utilized to further refine the initial segmentation. The robust matching algorithm is specifically designed to take advantage of general-purpose computation on graphics processing units, which reduces the execution time considerably. space represents a major Worldwide, is responsible according to the WHO

In the case of high density pathologies (e.g., pneumonia), space segmentation becomes a nontrivial task, and frequently, conventional algorithms fail to deliver suitable segmentation results. Thus, to enable computer-aided planning Noise removal is important for the reliability of subsequent image analyses, and is often one major focus during the preprocessing stage in image processing. However, most existing image denoising methods are for analyzing 2D images. Some of them can be extended to 3D cases, but their direct extensions may not be able to handle 3D images efficiently because the structure of a typical 3D image is often substantially more complicated than that of a typical 2D image. For instance, edge locations are surfaces in 3D cases which have much more complicated structures (e.g., intersections of two edge surfaces, pointed corners, and so forth) compared to edge curves in 2D cases. Of course, a 3D image can also be denoised by first dividing the 3D image into slices of 2D images and then applying 2D image denoising procedures to the 2D slices. But, it would not be efficient to denoise 3D images in that way because the 3D spatial information is not used efficiently when denoising individual 2D images. Besides noise removal, another important requirement for image denoising procedures is that they should preserve important image structures such as edges and major edge features.

Zhang, Y., Brady, M., Smith, S., et al, have proposed Researchers have applied various techniques to enhancing the interaction between humans and computers through the use of emotion recognition; however, one of the most common forms of such applications is based on a neural network. A neural network incorporates six fundamental human emotions: disgust, anger, fear, happiness, sadness, surprise, and neutral and uses them as a ground for emotional detection. These techniques were used when they developed their "Humanoid Robots". "Humanoid Robots" was developed on the bases of Generalised Feed Forward Neural Network (GFFNN) and Multilayer Perceptron (MLP) for the classification stage while the Statistical Parameters and Discrete Cosine Transform (DCT) have been used for feature extraction. This report has achieved approximately 100% accuracy rate regarding testing and training data. Whereas the intelligent robot, that is implemented to achieved 92% accuracy. In several techniques when building their robot. The Principal Component Analysis (ACP) and the Harr Wavelet Transform have been used for extracting facial features while the nonlinear Support Vector Machine (SVM) and Euclidean distance technique have been used for the classification of emotions. However, both of these reports are similar in that they are superior to the grayscale images.

3. PROPOSED WATERSHED SEGMENTATION TECHNIQUE

In this section, introduced that includes 4 steps i.e. data acquisition, image enhancement, image segmentation and the last step is feature extraction and Paddy identification.

Data acquisition is the process of sampling signals that measure real world physical conditions and converting the resulting samples into digital numeric values that can be manipulated by a computer. Data acquisition systems (abbreviated with the acronym **DAS** or **DAQ**) typically convert analog waveforms into digital values for processing. The components of data acquisition systems include:

- Sensors that convert physical parameters to electrical signals.
- Signal conditioning circuitry to convert sensor signals into a form that can be converted to digital values.
- Analog-to-digital converters, which convert conditioned sensor signals to digital values.

Image enhancement is the process of adjusting digital images so that the results are more suitable for display or further analysis. For remove noise or brighten an image, making it easier to identify key features. It perform image enhancement in MATLAB with Image

Processing Toolbox, which provides algorithms for image enhancement, including, The filtering and feature extraction stage is the most significant stage that develops a successful emotion recognition system. There are a huge raw data on the facial images and we need to filter and feature the extraction stages; this is the most significant stage to develop successful emotion recognition system. There are a huge raw data on the facial image and it need to analyse them and limit these data to a small set of information called a feature space. The effective and efficient performance analysis depends on the quality of the feature space. Thus, it is required to use a smaller relevant data set that is extracted from images rather than uses the whole original data. Additionally it is useful to use hybrid approaches that combine Appearance features and Geometric features. In past and current researches, there is no convincing evidence that proves the existence of one optimal solution. However, there are proofs that the best choice is unquestionably the use of a hybrid approach. Therefore, the optimal solution will be measured by which suitable combination approaches come together to improve the accuracy of emotion recognition system performance.

Some approaches of Filtering and Feature extraction that have used image processing in general as well as emotion recognition systems in particular will be presented in the following sections. These data are analyzed and limited to small sets of information called feature space..

Filtering and Feature Extraction Stage

The filtering and feature extraction stage is the most significant stage that develops a successful emotion recognition system. There are a huge raw data on the facial images and we need to filter and feature the extraction stages; this is the most significant stage to develop successful emotion recognition system. There are a huge raw data on the facial image and it need to analyse them and limit these data to a small set of information called a feature space. The effective and efficient performance analysis depends on the quality of the feature space. Thus, it is required to use a smaller relevant data set that is extracted from images rather than uses the whole original data.

Recently, many image-processing researches have been carried out in order to produce effective features that distinguish between the seven basic facial expressions; each approach is based on a specific area of analysis for feature extraction. For example, some approaches extract feature information dependent on geometric features that are based on two-dimensional or three-dimensional facial images; mouth, eyes, and eyebrows. Whereas other approaches are based on static image information; this type of approach extracts features by filtering the image. The acquired features are

called Appearance features. Several filter images can be used, for example, Principal Component Analysis (PCA), Independent Component Analysis (ICA), Discrete Cosine Transform (DCT), Gabor Filters, Fast Fourier Transform (FFT), Singular Value Decomposition (SVD), Harr Wavelet transforms and Integral Image Filter etc. In several cases, multiple techniques and filtering of extracted features are used together to achieve better performance. Additionally it is useful to use hybrid approaches that combine Appearance features and Geometric features. In past and current researches, there is no convincing evidence that proves the existence of one optimal solution. However, there are proofs that the best choice is unquestionably the use of a hybrid approach. Therefore, the optimal solution will be measured by which suitable combination approaches come together to improve the accuracy of emotion recognition system performance.

Some approaches of Filtering and Feature extraction that have used image processing in general as well as emotion recognition systems in particular will be presented in the following sections. These data are analyzed and limited to small sets of information called feature space. The effective and efficient performance analysis is dependent on the quality of feature space. Thus, it is required to use a smaller more relevant data set that is extracted from the image rather than to use the entire original.

Image segmentation is the process of dividing an image into multiple parts. This is typically used to identify objects or other relevant information in digital images. Transform methods, such as watershed segmentation method.

4. DIFFERENTIAL ANALYSIS

Kidney stone analysis uses one or more test methods to examine and determine the composition of a stone from the urinary tract. This is done in order to help identify the cause of the stone and, where possible, to prevent the formation of more stones.

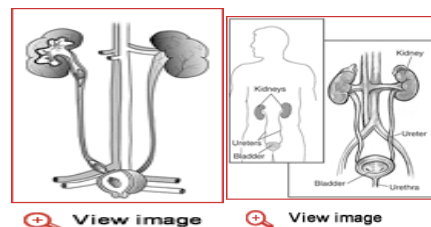


Fig: 3.1: Cross section view of kidney

The urinary tract consists of two kidneys, two ureters, the bladder, and the urethra. The kidneys filter wastes out of the blood and produce urine, which is

transported from the kidneys to the bladder through tube-like ureters. Urine is eliminated from the bladder through the urethra. This is a continual process of waste filtration, urine production, and elimination.

Commonly called kidney stones, urinary tract stones or calculi can form in the kidneys and in other parts of the urinary tract. Kidney stones can cause problems either because they grow large enough to obstruct urine flow or because they become dislodged or break off and begin to travel from a kidney through the ureter; they can cause temporary obstruction and stretch, irritate, and/or damage the walls of the ureters. This movement can cause abrupt, extremely severe pain that may be intermittent or continuous.

Many stones will eventually pass out of the body in the urine, but some are too large or have too irregular a shape for the body to expel. With very large stones, which typically cannot pass from the kidney into the ureters, and for smaller stones that get into but do not pass through the ureters, some form of treatment is needed. The stone may need to be surgically removed, often using devices that pass through the urethra and bladder to the site of the stone. With some stones, it is possible to use extracorporeal shock wave lithotripsy. This treatment pulverizes the stone in place using targeted shock waves. The smaller particles and fragments that remain can then pass through the urinary tract.

Stones can develop for several reasons, but the most common is because there is a high concentration of a particular chemical in the urine that precipitates and forms crystals. This can happen when a person produces and excretes an excess amount of the chemical. It can also occur when a person chronically takes in little liquid and has a more concentrated urine because there is less water in it. Depending on how much and what type of material crystallizes and where it forms, a kidney stone may be round, sharp and pointy or irregular with branches (called a staghorn). It can range in size from a grain of sand to bigger than a golf ball.

The composition of the stone depends upon the chemicals present in excess. It may be all one chemical compound or have different chemicals in different layers.

Common types of kidney stones include:

- Calcium oxalate
- Calcium phosphate
- Uric acid
- Struvite (magnesium ammonium phosphate) - stones associated with a bacterial infection

ssThese four types make up about 95% to 99% of kidney stones. About 75% of stones will contain calcium. Less common stones include:

- Cystine - stones associated with an inherited excess of cystine excretion

- Drug-related - stones that are associated with drugs such as guaifenesin, indinavir, triamterene, atazanavir, and sulfa drugs.

According to the National Institute of Diabetes and Digestive and Kidney Diseases, kidney stones are one of the most common urinary tract disorders. In the U.S., about half a million people go to the emergency room each year with kidney stones and about three million visit their doctor.

5. WATERSHED SEGMENTATION

The watershed transform is a well-established image-processing technique for grey-scale images. It is based on topographical interpretation of the gradient image. The density magnitude is considered as a topographical relief, where the brightness value of each voxel corresponds to physical elevation. The water flowing down the elevation is always following the gradient direction (direction with maximal density change) to the nearest local minimum. Areas with common local minimum constitute watershed regions, and the borders between these regions constitute the watersheds. Vincent and Soille showed that an alternative of the watershed transform as an immersion algorithm is also possible. The procedure results in partitioning of the image in catchment basins, the borders of which define the watersheds. In this way, watershed algorithms create closed borderlines, which can be used for segmentation. A common problem of watershed algorithms is over segmentation. Due to noise and randomness of natural medical data, the volume is partitioned into innumerable small regions. By low-pass filtering of the data (e.g. by the means of a Gaussian filter) it is possible to reduce the number of unimportant details and to reduce the number of regions. The disadvantage of this approach is that the borders of the regions are shifted (due to the nature of low-pass filtering) and become imprecise. Hierarchical merging of regions has been suggested as a solution in this case. Alternatively, regions can be merged based on their statistical attributes

The watershed transform is often applied to this problem. The watershed transform finds "catchment basins" and "watershed ridge lines" in an image by treating it as a surface where light pixels are high and dark pixels are low.

Segmentation using the watershed transform works better if you can identify, or "mark," foreground objects and background locations. Marker-controlled watershed segmentation follows this basic procedure:

1. Compute a segmentation function. This is an image whose dark regions are the objects you are trying to segment.

2. Compute foreground markers. These are connected blobs of pixels within each of the objects.

3. Compute background markers. These are pixels that are not part of any object.

4. Modify the segmentation function so that it only has minima at the foreground and background marker locations.

5. Compute the watershed transform of the modified segmentation function.

Morphological Gradient

The morphological gradient g of a function f is defined by

$$g(f) = [(f \circ H) - (f \circ S)]$$

where $(f \circ S)(x) = \text{Sup}(f(y))$ is the dilation of f at the point x .

and $(f \circ H)(x) = \text{Inf}(f(y))$ is the erosion of f (where H is the elementary hexagon on an hexagonal grid).

Watershed transformation

The watershed transformation is more complex. Let us give an intuitive definition of this operation by considering the graph of f as a topographic surface. This surface presents minima, which are connected regions where it is not possible to reach a point at a lower altitude by an always descending path. Suppose that minima are pierced and that the topographic surface is immersed in water. The water will pour through the hole through the deepest ones at first, and will progressively flood the surface. While flooding, we build dams at any point where waters coming from two different minima may merge. At the end of the flooding, divide lines appear, called watersheds of the function f . The different connected components separated by the watershed lines are called catchment basins, each one being associated to a single minimum.

Markers Oriented Segmentation

If the principle of the segmentation by a simple watershed of the gradient is appealing, the results aren't. Noise and inhomogeneities produce a lot of minima which lead over-segmentation of the image.

The procedure can be enhanced if we define new markers for the objects to be extracted. These markers are obtained by various means, which will be discussed later. These markers are then imposed as the new minima of the gradient. Doing so, we modify the gradient function as a result, the only minima of this modified gradient are the imposed markers. This modified function nevertheless, is close enough to the original gradient function to preserve the edges, this modification is performed with geodesic image reconstruction

Segmentation with regularized gradient.

The main advantage of the regularized gradient is its ability to take into account the variations of the initial function. This first segmentation can

now be used for extracting a coarse marker of the road. This marker is obtained by selecting the catchment basin of $W(g^*)$ located at the front of the area. This marker is smoothed and an outer marker is built in order to mark the region of the image which do not belong to the area.

Segmentation Using a Simplified Image

Portion markers are obtained by image simplification. A simplified image is obtained from the image f and its gradient $g(f)$.

Let's consider the minima M of g and let's define a function h as follow:

$$h = f \cdot k$$

Let's compute the geodesic reconstruction of h by dilation inside the catchment basins. This operation produces an image where each basin of g is valued. This valuation leads to a simplified image f made of tiles of constant grey values. This image is called the mosaic-image.

The gradient of this mosaic-image may be defined. This gradient will be null every where except on the divide lines of g where it is equal to the absolute difference between of the grey-tone values of the catchment. The watersheds of this function point out the regions of the image surrounded by higher contrast edges. Compare the results of these two algorithms with the one with the regularized gradient. We can still extract a marker for the road, and use it to modify the gradient image.

The second order information (Hessian) has an intuitive justification in the context of vessel detection. λ_k will be the eigen value with the k -th smallest magnitude ($|\lambda_1| \leq |\lambda_2| \leq |\lambda_3|$). Under this assumption Table 1 summarizes the relations that must hold between the eigenvalues of the Hessian for the detection of different structures. In particular, a pixel belonging to a vessel region will be signaled by λ_1 being small (ideally zero), and λ_2 and λ_3 of a large magnitude and equal sign (the sign is an indicator of brightness/darkness). We are interested in "vesselness" measures suited for medical images. In CT, vessels emerge as bright tubular structures in a darker environmental

$$\begin{aligned} |\lambda_1| &\approx 0 \\ |\lambda_1| &< |\lambda_2| \\ \lambda_2 &\approx \lambda_3 \end{aligned}$$

and the sign of λ_2 and λ_3 indicate its polarity.

Our dissimilarity measure takes into account two geometric ratios based on the second order ellipsoid. The first ratio accounts for the deviation from a blob-like structure but cannot distinguish between a line- and a plate-like pattern:

$$RB = \frac{\text{Volume}/(4\pi/3)}{|\lambda_1|} =$$

$$\frac{(\text{Largest Cross Section Area}/\pi)^{3/2}}{\sqrt{|\lambda_2\lambda_3|}}$$

This ratio attains its maximum for a blob-like structure and is zero whenever $\lambda_1 \approx 0$, or λ_1 and λ_2 tend to vanish (notice that λ_1/λ_2 remains bounded even when these eigenvalue is very small since its magnitude is always larger than the first).

The second ratio refers to the largest area cross section of the and accounts for the aspect ratio of the two largest second order derivatives. This ratio is essential for distinguishing between plate-like and line-like structures since only in the latter case it will be zero,

$$\text{RA} = \frac{(\text{Largest Cross Section Area})/\pi}{\frac{|\lambda_2|}{(\text{Largest Axis Semi-length})^2} |\lambda_3|}$$

The two geometric ratios we introduced so far are grey-level invariant (i.e., they remain constant under intensity re-scalings). This ensures that our measures only capture the geometric information of the image. However, in CT images there is additional knowledge available: vessel structures are brighter than the background and occupy a (relatively) small volume of the whole dataset. If this information is not incorporated background pixels would produce an unpredictable filter response due to random noise fluctuations. However, a distinguishing property of background pixels is that the magnitude of the derivatives (and thus the eigenvalues) is small, at least for typical signal-to-noise ratios present in acquired datasets.

Edge detection, sharpening, and luminance filtering are common operations in image processing. They mainly involve arithmetic operations and exhibit much parallelism. GPU is ideal for such operations, because GPU has multiple floating points processing units running in parallel. Note that the third step responses to the local appearance model matching, and its purpose is to find the best location of the feature point by matching the profile of the feature point to the training result. After the GPU-based preprocessing, the edge in the sketch image is much stronger than that in the original gray-level image, so the local appearance model matching process more quickly converges. In addition, to further improve facial expression recognition accuracy based on image ratio features, we combine image ratio features with Facial Animation Parameters (FAPs), which describe the geometric motions of facial feature points. In addition to feature point motions, facial expressions exhibit image intensity changes due to skin deformations (e.g., facial creases and wrinkles). These are important visual cues for human perception. To capture such information, we introduce SDPs (Skin Deformation Parameters).

A watershed is formed by ‘flooding’ an image from its local minima, and forming ‘dams’ where waterfronts meet. When the image is fully flooded, all

dams together form the watershed of an image. The watershed of an edge ness image (or, in fact, the watershed of the original image) can be used for segmentation. The idea is that when visualizing the edgeness image as a three dimensional landscape, the catchment basins of the watershed correspond to objects, that the watershed of the edgeness image will show the object boundaries. As the landscape in the catchment basins, the small defects because of image artifacts. Because of the way the watershed is constructed –it forms ‘dams’ where waterfronts meet– these small defects do not disturb the watershed segmentation much pre- and post-processing of the watershed image is needed to obtain a good segmentation. Usual post-processing is the filling in of the boundaries to obtain 304 Segmentation solid segments. In the case of watershed segmentation do not need to worry about small ‘leaks’ in a boundary (a small leak between two segments will fill in the two segments as being a single segment). Because of the way the watershed is constructed.

Objects are surrounded by a ‘palisade’, that will hold the water in the flooding process that form the watershed. Dams will be formed when the water level reaches the tops of the palisades.

An uneven palisade height will not disturb the formation of the correct dam marking an object boundary. Bottom right: all dams formed; the watershed of the edgeness image. Some pre- and post-processing is usually necessary to avoid an oversegmentation. Since such dams are caused by very weak edges, they are unlikely to correspond to object boundaries, and should not be part of the segmentation watershed. It still shows some over segmentation besides the correct object boundaries, several erroneous branches are present.

Many approaches have been proposed to remove these erroneous branches. One effective method is to merge those segments that are likely to belong together. It is measured is discussed in the section on region based segmentation.

In 3D cases, it need to describe three major features of the edge surfaces: 1) planar parts, 2) intersections of two planar edge surfaces, and 3) pointed corners. To describe these three major features, consider the family of three basic surface templates shown in the first row and the left panel of the second row of among them, the plane is used for approximating planar parts of the edge surfaces, the intersection of two half planes is for approximating roofs/valleys of the edge surfaces, and the cone is for approximating pointed corners.

Edge surface approximation by the surface templates is proposed by algorithm is given as follows. At a given voxel (x,y,z) , let us consider its spherical neighborhood $O(x,y,z)$ with radius h_n . Let $\{s_i; i = 1, 2, \dots, m\}$ be the detected edge voxels in $O(x,y,z)$, $\{\beta_i; i = 1, 2, \dots, m\}$ be the corresponding estimated gradient

directions (with unit lengths) at these edge voxels. G is a weighted second moment from origin of β_i , and the weights are determined by the significance of individual detected edge voxels. The eigenvalues of G are denoted as $\lambda_1 \leq \lambda_2 \leq \lambda_3$, and the corresponding eigenvectors with unit lengths are v_1, v_2 , and v_3 . Then, if all β_i s are the same (i.e., the underlying edge surface is a plane), G would have a rank of 1 and v_3 would be the normal direction of the edge plane, and vice versa. Therefore, to approximate the edge surfaces in $O(x,y,z)$ by the first surface template shown in Fig., a reasonable solution is the plane that passes the weighted center s of $\{s_i\}$ with the weights $\{w_i\}$ and has the normal direction of v_3 .

To approximate the edge surfaces in $O(x,y,z)$ by the second surface template proceed in two steps. First, $\{s_i\}$ are divided into two groups by a plane that passes s along the directions of v_1 and β_1^* , where β_1^* denotes the weighted average of $\{\beta_i; i = 1, 2, \dots, m\}$ with the weights $\{w_i; i = 1, 2, \dots, m\}$. Second, with each group of the detected edge voxels, find an approximation plane passing their weighted averaged locations with its normal direction to be the weighted average of the estimated gradient directions at the detected edge voxels. Then, the two resulting half planes that cross each other and form a subspace in $O(x,y,z)$ containing s are used for approximating the edge surfaces in $O(x,y,z)$.

To approximate the edge surfaces in $O(x,y,z)$ by a cone need to specify its central axis, vertex position, and the angle between the central axis and any generatrix. To specify the location of the central axis, let us consider a sphere $O'(x,y,z)$ of radius $hn' > hn$. The plane P passing s with the normal direction of d would divide $O'(x,y,z)$ into two parts. Weighted centers of the detected edge voxels in the two parts are then calculated, and the one closer to P is denoted as $s^* = (c_x^*, c_y^*, c_z^*)$. Then, the line passing s^* along direction d is defined to be the central axis of the cone. After the central axis is determined, the angle between the central axis and any generatrix can be easily estimated by the weighted average of the angles between d and $\{\beta_i; i = 1, 2, \dots, m\}$. The location of the vertex (v_x, v_y, v_z) of the cone can be estimated by minimizing the weighted orthogonal distance between the cone and the detected edge voxels in $O(x,y,z)$.

It need to choose one of the four estimated surface templates based on observed image intensities for approximating the edge surfaces in $O(x,y,z)$. For that purpose, one natural solution is to choose the estimated surface template with the smallest residual sum of squares (RSS), where RSS is defined to be the sum of squared orthogonal distances from detected edge voxels s_i to the estimated surface template. However, by this idea, the first surface template would never be selected because it is a special case of the second surface template and, consequently, its RSS value will never be the smallest one.

ALGORITHM

➤ PCA ALGORITHM is used

3.5.1 Principal Components Analysis

Real-world data sets usually exhibit relationships among their variables. These relationships are often linear, or at least approximately so, making them amenable to common analysis techniques. One such technique is principal component analysis ("PCA"), which rotates the original data to new coordinates, making the data as "flat" as possible.

Given a table of two or more variables, PCA generates a new table with the same number of variables, called the principal components. Each principal component is a linear transformation of the entire original data set. The coefficients of the principal components are calculated so that the first principal component contains the maximum variance (which we may tentatively think of as the "maximum information"). The second principal component is calculated to have the second most variance, and, importantly, is uncorrelated (in a linear sense) with the first principal component. Further principal components, if there are any, exhibit decreasing variance and are uncorrelated with all other principal components.

3.5.2 Discussion

PCA "squeezes" as much information (as measured by variance) as possible into the first principal components. In some cases the number of principal components needed to store the vast majority of variance is shockingly small: a tremendous feat of data manipulation. This transformation can be performed quickly on contemporary hardware and is invertible, permitting any number of useful applications. For the most part, PCA really is as wonderful as it seems. There are a few caveats, however:

1. PCA doesn't always work well, in terms of compressing the variance. Sometimes variables just aren't related in a way which is easily exploited by PCA. This means that all or nearly all of the principal components will be needed to capture the multivariate variance in the data, making the use of PCA moot.

2. Variance may not be what we want condensed into a few variables. For example, if we are using PCA to reduce data for predictive model construction, then it is not necessarily the case that the first principal components yield a better model than the last principal components (though it often works out more or less that way).

3. PCA is built from components, such as the sample covariance, which are not statistically robust. This means that PCA may be thrown off by outliers and other data pathologies. How seriously this affects the result is specific to the data and application.

4. Though PCA can cram much of the variance in a data set into fewer variables, it still requires all of the variables to generate the principal components of future observations. Note that this is true, regardless of how many principal components are retained for the application. PCA is not a subset selection procedure, and this may have important logistical implications.

5. Noise removal is important for the reliability of subsequent image analyses, and is often one major focus during the preprocessing stage in image processing. Besides noise removal, another important requirement for image denoising procedures is that they should preserve important image structures such as edges and major edge features (e.g., intersections of two edge surfaces, pointed corners, and so forth).

6. Most of the existing image denoising procedures can preserve parts of the edges where the curvature of edge surfaces is relatively small, but would usually blur or round certain edge features at places where the curvature of edge surfaces is relatively large. Edge features corresponding to relatively large curvature of the edge surfaces are an important component of the image under study because they often represent major characteristics of the image objects and are easier to capture our visual attention compared to places on the edge surfaces with relatively small curvature. Therefore, they should be well preserved during image denoising.

7. A new 3D image denoising procedure is proposed which can preserve edges and major edge features well. Compared to most existing 3D image denoising procedures, we make the following two innovations in our method: First, we propose detecting edge voxels and then approximating the underlying edge surfaces locally based on the detected edge voxels by a surface template chosen from a prespecified surface template family. The surface template family is specified in a way that major features of the edge surfaces can be accommodated well by its surface templates, which makes it possible for us to preserve edges and major edge features in 3D image denoising.

8. As a comparison, some existing 2D/3D methods control the amount of data smoothing around a given pixel/voxel based on the estimated gradient of the underlying image intensity function, and the estimated gradient cannot distinguish different edge structures well. Some other methods (e.g., the kernel smoothing method) try to preserve edges by locally approximating the edge curves/surfaces by straightlines/planes. By these methods, pointed corners and other structures with large curvature cannot be preserved well. Second, we use certain jump regression analysis (JRA) methodologies in proposed image denoising procedure.

9. Under the JRA framework, the image denoising problem can be regarded as a special nonparametric regression problem discussed in the statistical literature, where the image intensity function is

regarded as a jump regression function with jumps at the edge locations. Then, image denoising can be accomplished by estimating the regression function with jumps preserved. One benefit to adopting the JRA framework is that some local smoothing methodologies developed in the statistical literature can be used for image denoising. Such local smoothing methods have flexibility in choosing proper windows and in assigning proper weights for efficient local weighted averaging, which is helpful for different tasks in image processing

Step 1: Read in the Color Image and Convert it to Grayscale

Step 2: Use the Gradient Magnitude as the Segmentation Function

Use the Sobel edge masks, `imfilter`, and some simple arithmetic to compute the gradient magnitude. The gradient is high at the borders of the objects and low (mostly) inside the objects.

Step 3: Mark the Foreground Objects

A variety of procedures could be applied here to find the foreground markers, which must be connected blobs of pixels inside each of the foreground objects. In this example you'll use morphological techniques called "opening-by-reconstruction" and "closing-by-reconstruction" to "clean" up the image. These operations will create flat maxima inside each object that can be located using `imregionalmax`.

2erosion followed by a morphological reconstruction. Let's compare the two. First, compute the opening using `imopen`.

Following the opening with a closing can remove the dark spots and stem marks. Compare a regular morphological closing with a closing-by-reconstruction. First try `imclose`:

Now use `imdilate` followed by `imreconstruct`. Notice you must complement the image inputs and output of `imreconstruct`.

Comparing `Iobrcbr` with `Ioc`, reconstruction-based opening and closing are more effective than standard opening and closing at removing small blemishes without affecting the overall shapes of the objects. Calculate the regional maxima of `Iobrcbr` to obtain good foreground markers.

To help interpret the result, superimpose the foreground marker image on the original image.

Notice that some of the mostly-occluded and shadowed objects are not marked, which means that these objects will not be segmented properly in the end result. Also, the foreground markers in some objects go right up to the objects' edge.

This procedure tends to leave some stray isolated pixels that must be removed. Can do this using `bwareaopen`, which removes all blobs that have fewer than a certain number of pixels.

Step 4: Compute Background Markers

The background pixels are in black, but ideally don't want the background markers to be too close to the edges of the objects we are trying to segment. Will "thin" the background by computing the "skeleton by influence zones", or SKIZ, of the foreground of bw. This can be done by computing the watershed transform of the distance transform of bw, and then looking for the watershed ridge lines (DL == 0) of the result.

Step 5: Compute the Watershed Transform of the Segmentation Function.

The function imimposemin can be used to modify an image so that it has regional minima only in certain desired locations. Here you can use imimposemin to modify the gradient magnitude image so that its only regional minima occur at foreground and background marker pixels.

Finally we are ready to compute the watershed-based segmentation.

Step 6: Visualize the Result

One visualization technique is to superimpose the foreground markers, background markers, and segmented object boundaries on the original image. It can use dilation as needed to make certain aspects, such as the object boundaries, more visible. Object boundaries are located where L == 0.

This visualization illustrates how the locations of the foreground and background markers affect the result. In a couple of locations, partially occluded darker objects were merged with their brighter neighbor objects because the occluded objects did not have foreground markers.

Another useful visualization technique is to display the label matrix as a color image. Label matrices, such as those produced by watershed and bwlabel, can be converted to truecolor images for visualization purposes by using label2rgb.

5. RESULT AND DISCUSSION

This system illustrates how to implement the designed system that is explained in the previous chapter (Chapter 4: Design) which discusses the implementation strategies and the usage tool that are employed to develop this project. This chapter highlights whether the implemented functions are open source functions or functions written by the author. Finally, the testing procedure that is required to assess the implemented project is clarified at the end of this chapter. **SCREEN**



SHOOT:

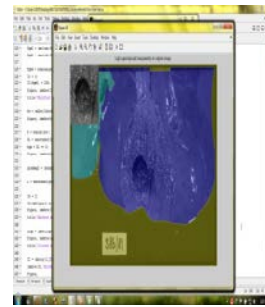


Figure.1:InputImageResolution 300DPI

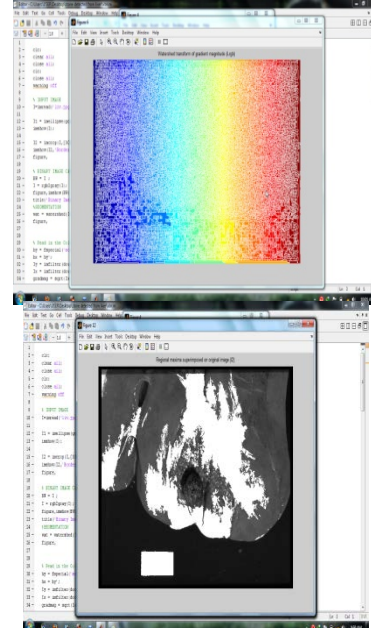


Figure.3: Watershed ImageResolution 300DPI

Figure.4: Superimpose the foreground marker image on the original image.Resolution300DPIThe performance, Comparisons of the different Segmentation method is shown in below table

Category	Thresholding methods	Clustering methods	Transform methods
Object	0.8592	0.8071	0.8919
Nature	0.8275	0.8301	0.8995
Human	0.7750	0.7750	0.8163
Animal	0.8236	0.8796	0.8984

Table 1: Comparison of various Segmentation methods (in Mean values) From the table, can analysis the

performance of the different types of segmentation method.

Here Thersholding, Clustering, and Transform method Segmentation methods are analysed..

6. CONCLUSION

PCA is an analytical tool for differentiation of different types of human kidney stones, and is especially useful for the negative ESI-MS mass spectral fingerprints in the analysis and detection of melamine-induced kidney stones. Melamine, a basic compound, could not be detected in the negative ESI mass. In this paper Watershed Segmentation methods are used, which produce the efficient segmentation compare to others. It can removed the portions, where as other methods can not removed.

REFERENCES

[1] Preminger GM (2010). Dual-Energy computed tomography with advanced postimage acquisition data processing: improved determination of urinary stone composition. *J. Endourol.*, 24: 47-354.

[2] Herring LC (1962). Observations on the analysis of ten thousand urinary calculi. *J. Urol.*, 88: 545-562.

[3] Hiatt RA, Ettinger B, Caan B, Quesenberry CP, Duncan JD, Citron JT (1996). Randomized controlled trial of a low animal protein. High Fiber Diet in the Prevention of Recurrent Calcium Oxalate Kidney Stones, 144: 25-33.

[4] Hu B, Peng XJ, Yang SP, Gu HW, Chen HW, Huan YF, Zhang TT, XL Qiao (2010). Fast quantitative detection of cocaine in beverages using nanoextractive electrospray ionization tandem mass spectrometry. *J. Am. Soc. Mass Spectrom.*, 21: 290-293.

[5] Jackson JE (1980). Principal components and factor-analysis. 1. Principal components. *J. Qual. Tech.*, 12: 201-213.

[6] Jia LQ, Shen Y, Wang XM, He LJ, Xin Y, Hu YX (2009). Ultrasonographic diagnosis of urinary calculus caused by melamine in children. *Chin. Med. J.*, 122: 252-256.

[7] Johnson CM, Wilson DM, O'fallon WM, Malek RS (1979). Renal Stone Epidemiology: A 25-Year Study in Rochester. Minnesota. *Kidney Int.*, 16: 624-631.

[8] Lam CW, Lan L, Che XY, Tam S, Wong SY, Chen Y, Jin J, Tao SH, Tang XM, Yun KY, H PK (2009). Diagnosis and spectrum of melamine-related renal disease: Plausible mechanism of stone formation in humans. *Clin. Chim. Acta.*, 402: 150-155.

[9] Evan AP, Coe FL, Lingeman JE, Worcester E (2005). Insights on the pathology of kidney stone formation. *Urol. Res.*, 33: 383-389. Ferrandino MN, Pierre SA, Simmons WN, Paulson EK, Albala DM.

[10] Moe OW (2006). Kidney stones: path physiology and medical management. *The Lancet*, 367: 333-344.

[11] Otnes B (1983). Urinary stone analysis methods, materials and value. *Scand. J. Urol. Nephrol. Suppl.*, 71: 1-109.

[12] Sodhi RNS, Chen HW, Yang SP, Hu B, Zeng X, Xiao RH (2010). TOF-SIMS analysis of kidney stones possibly induced by the ingestion of melamine-containing milk products. *Surf. Interface Anal.*,

[13] Bankman I.N., editor, *Handbook of Medical Imaging, Processing and Analysis*. Academic Press, 2000.,

[14] Warfield, S.K., Zou, K.H., Wells, W.M., "Simultaneous Truth and Performance Level Estimation (STAPLE): An Algorithm for the Validation of Image Segmentation,

[15] Comaniciu and P. Meer, "Mean shift: A robust approach toward feature space analysis," *IEEE Trans. Pattern Anal. Mach. Intell.*, vol. 24, no. 5, pp. 603-619, May 2002.

[16] Zhang, Y., Brady, M., Smith, S., "Segmentation of brain MR images through a hidden Markov random field model and the expectation maximization algorithm," *IEEE Trans. on Medical Imaging*, vol. 20(1), pp 45-57, 2001.